A neutron diffraction study of oxygen and nitrogen ordering in a kinetically stable orthorhombic iron doped titanium oxynitride

On Ying Wu [a], Ivan P Parkin [a], Geoffrey Hyett [b],*

[a] Department of Chemistry, Materials Chemistry Research Centre, University College London, 20 Gordon Street, London, WC1H 0AJ, UK
[b] School of Chemistry, University of Leeds, Leeds, LS2 9JT, UK

ARTICLE INFO

ABSTRACT

The synthesis of a polycrystalline powder sample of iron doped orthorhombic titanium oxynitride, $Ti_{2.92}Fe_{0.01}O_{4.02}N_{0.98}$, on the scale of 0.7 g has been achieved. This was conducted by the unusual route of delamination from a steel substrate of a thin film deposited using atmospheric pressure chemical vapour deposition. The structure of the titanium oxynitride is presented, determined from a combined analysis of X-ray and neutron powder diffraction data. The use of neutron diffraction allows the position of the oxygen and nitrogen ions in the material to be reported unambiguously for the first time. In this study $Ti_{2.92}Fe_{0.01}O_{4.02}N_{0.98}$ is found to crystallise in the $Cmcm$ space group, iso-structural pseudobrookite, with lattice parameters $a = 3.81080(6)$ Å, $b = 9.6253(2)$ Å, and $c = 9.8859(2)$ Å, and contains partial oxygen–nitrogen ordering. Of the three anion sites in this structure one is exclusively occupied by oxygen, while the remaining two sites are occupied by oxygen and nitrogen in a disordered manner. Testing indicates that this iron doped titanium oxynitride is a metastable phase that decomposes above 700 °C into TiN and TiO_2, the thermodynamic products.

© 2012 Elsevier Inc. All rights reserved.

1. Introduction

Mixed anion solid state materials such as oxynitrides and oxychalcogenides are of interest to researchers because of the greater structural complexity that the additional anion allows, and the concomitant affect this has on the electronic structure and properties [1–4]. The importance of this research area has been highlighted by the recent identification of oxypnictides as high temperature superconductors [5].

The majority of solid state oxynitride phases are synthesised by reaction of an oxide precursor with either ammonia, at temperatures typically greater than 800 °C [3,6,7], or by direct reaction with nitrogen gas at even higher temperatures [8,9]. These approaches have successfully allowed the synthesis of a limited number of ternary transition metal oxynitrides, including those of titanium, vanadium, tungsten and niobium which adopt the $M(O_xN_y)$, $x + y = 1$, rock salt structure [10–12]. Others, such as Zr_2ON_2 and Hf_2ON_2 take the bixbyite structure [13]. Tantalum oxynitride, TaON, has been identified in two confirmed polymorphs taking the monoclinic baddeleyite and $VO_2(B)$ structures [14,15]. It has also been possible to synthesis oxynitrides using a non-oxide starting material in a reaction with water saturated

ammonia at 900–1000 °C such as the synthesis of Ta_3O_6N from TaS_2 and Zr_7O_8N from $ZrCl_4$ [16,17]. However, the high temperatures used in all these examples mean that only the thermodynamic products are accessible. Any metastable, kinetic products will be difficult to identify by these routes. In contrast, more recent examples of lower temperature syntheses have indentified both a vanadium and titanium oxynitride which do not adopt the long known and thermodynamically stable rock-salt structures. Instead these kinetically stable oxynitrides, $V_3O_{4.61}N_{0.27}$ and $Ti_{2.85}O_4N$, adopt the pseudobrookite-type structure [18,19].

The orthorhombic titanium oxynitride, $Ti_{2.85}O_4N$, was discovered using a novel technique based on chemical vapour deposition, carried out at 600 °C [18] whereby there was an initial deposition as a thin film, which was then delaminated to yield a powder from which the structure was determined by X-ray diffraction. The material has been determined to be a photocatalyst [20], and is also the subject of a high-pressure study [21]. The related oxide, Ti_3O_5, is found at room temperature to adopt a pseudobrookite-like structure which is monoclinic, but above 241 °C adopts the true, orthorhombic pseudobrookite structure [22]. It is this high temperature polymorph that is isostructural to $Ti_{2.85}O_4N$, which can therefore be considered a nitrogen for oxygen substituted form of Ti_3O_5, in which the substitution reduces the monoclinic to orthorhombic structural transition to below room temperature. Cationic substitution of the form

$M_xTi_{3-x}O_5$ where M=Li, Mg and Fe had been previously shown to also reduce the structural transition temperature so that the pseudobrookite structure was observed at room temperature [23–26]. For both cationic and anionic substitution it is lowering of the Fermi level that induces the structural change.

In the previously reported synthesis of $Ti_{2.85}O_4N$ the sample was made by delamination of a thin film from a glass substrate, producing a 25 mg sample for which the structure and composition were confirmed by XRD and XPS. However, there was still some uncertainty as to the presence of any oxygen or nitrogen ordering due to the similarity in X-ray scattering factor for the oxide and nitride ions. This was unfortunate because the similar size and polarizability of the oxide and nitride ions mean that they can occupy the same crystallographic sites, but structural complexity may still result depending on whether the two different ions are ordered or disordered across those sites. For example, most compounds with isotopic structures and similar anion sites (coordination number, bond lengths) show disordered occupation by oxygen and nitrogen, and these include perovskite structures, such as $LaAO_2N$, (A=Ti, Zr) $BaBO_2N$, (B=Ti, Zr) and $NdTiO_2N$, [8,27,28], or the bixbyite structured $ZrON_2$, in which all the anion are 4 coordinate [13]. Ordering of oxygen and nitrogen is more common in structures with different anion sites, such as in both β and γ TaON, containing mixtures of 3 and 4 and 2, 3 and 4 coordinate anion site, respectively. In each case nitrogen is preferentially found on the higher coordination number sites [14,15]. However ordering can also be found in isotopic structures like the perovskites $SrTaO_2N$ and $CaTaO_2N$ [29], if the synthesis temperature is sufficiently low to prevent randomisation. Neutron diffraction data provides the most reliable method to resolve the position of the oxide and nitride ions due to the significant difference in coherent neutron scattering power for the two elemental nuclei, unfortunately the previously prepared sample of $Ti_{2.85}O_4N$ was of insufficient mass to conduct a neutron experiment.

In this paper a modified synthesis of the titanium oxynitride is presented making use of a steel rather than glass substrate. This has allowed the production of a much larger sample size upon which neutron diffraction experiments have been conducted, the analysis of which has allowed the presence of partial oxygen–nitrogen ordering to be observed. Portions of this sample have also been tested for thermodynamic stability in air and vacuum up to 1000 °C, the results of which will indicate that the traditional high temperature synthetic methods of nitridation would not be suitable in the synthesis of this titanium oxynitride.

2. Experimental methods

A thin film of the titanium oxynitride was synthesised using a cold walled atmospheric pressure chemical vapour deposition reactor, of which details have previously been published [18]. Titanium (IV) chloride (Aldrich 99.9%), ethyl acetate (BDH, GPR grade) and ammonia (BOC, anhydrous) were used as precursors and sources of titanium, oxygen and nitrogen. Titanium (IV) chloride and ethyl acetate were supplied from bubblers heated to 82 °C and 37 °C and transported using N_2 (BOC, oxygen free) carrier gas flows of 1.0 dm^3 min^{-1} and 0.5 dm^3 min^{-1}, respectively. The ammonia was supplied under its own vapour pressure at a rate of 0.2 dm^3 min^{-1}. An additional plain flow of N_2 at a rate 12 dm^3 min^{-1} was added as a diluent to the precursor laden gas flows at the point where they were combined before entry into the reactor. The deposition took 15 min and was carried out onto a stainless steel substrate of dimensions 90 × 227 × 0.5 mm^3, held at a temperature of 650 °C.

The use of a steel substrate allowed complete delamination of the film as the coated steel was flexed causing the brittle ceramic coating to peel off the surface. The fragments of film were then collected and ground in an agate pestle and mortar. This yielded 0.7 g of a dark-green powder.

Neutron diffraction was carried out with this powder sample using the *GEM Xpress* service on the GEM time-of-flight instrument at the ISIS pulsed neutron facility [30]. The data were collected using 6 banks of detectors covering scattering angles of 9–154°. The data were used in a Rietveld refinement carried out with the EXPGUI interface for the GSAS suite of software packages [31,32]. Additionally powder X-ray diffraction data were collected using a Bruker D8 instrument, utilising Cu K_α radiation. Scanning electron microscope imaging and energy dispersive X-ray analysis measurements were conducted using a JEOL 6301 field emission SEM.

After the neutron experiment had been concluded 0.025 g portions of the sample were tested for thermodynamic stability in air and under vacuum. For the air stability test the samples were placed in alumina crucibles and heated in a furnace for 48 h. For the vacuum stability test the samples were sealed using a dynamic vacuum in silica ampoules under a pressure of less than 10^{-2} mbar, then the ampoules placed in a furnace for 48 h. Both air and vacuum experiments were carried out at eight temperatures from 300 °C to 1000 °C at 100 °C intervals. After firing all samples were analysed using X-ray powder diffraction.

3. Results and discussion

A powder sample of titanium oxynitride was derived from a single delaminated film deposited onto a steel substrate by CVD from titanium(IV) chloride, ethyl acetate and ammonia. This produced a powder sample of 0.7 g, considered sufficient for a neutron diffraction experiment, carried out on the GEM instrument at the ISIS neutron source. It was also analysed using SEM and EDX.

3.1. SEM analysis

During the synthesis the adventitious difference in malleability of the synthesised compound and the steel substrate was used to completely delaminate the film and procure a sufficient quantity of powder product for a neutron diffraction experiment. However this method did lead to concern about contamination of the product with iron from the stainless steel substrate. In order to determine if iron was present in the film, energy dispersive X-ray analysis measurements were carried out using an SEM instrument. Iron contamination was a particular concern with this compound because monoclinic Ti_3O_5 can also be stabilised in its orthorhombic pseudobrookite form by cationic substitution of iron, as opposed to the anionic substitution targeted in this work – with Fe_2TiO_5 being pseudobrookite itself.

Energy dispersive X-ray spectra were collected from 16 spots on different powder particles, and additionally four wide area scans, each across a number of powder particles, were taken. The area analysis gave an average iron content of 1.6(4) % of the total metal content, while the average from the spot analysis was 1.8(6)%. This indicates that some contamination from the substrate did occur, in contrast to the initial work in which glass substrates were used, for which XPS measurements recorded that no other metals were present within the detection limit of the technique (< 0.5%). This small presence of iron, however, is not likely to be a controlling factor in determining the structure. The *Cmcm* structure for $Ti_{3-x}Fe_xO_5$ is only stable at room temperature with an iron content of above $x > 0.3$, or 10% metal basis, as such
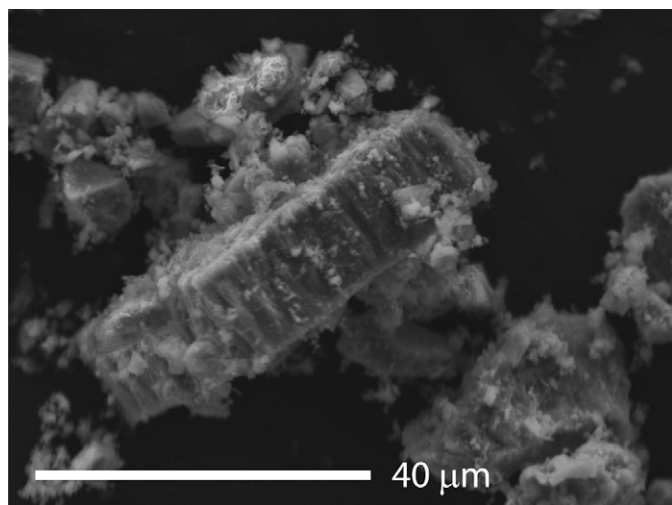
Fig. 1. SEM image of a particle of iron doped titanium oxynitride synthesised by APCVD. The image shows the broken edge of a piece of the original film.

we can be certain that it is still the presence of the nitrogen that dominates the structure direction in the material discussed here.

SEM imaging was also conducted and an example image can be seen in Fig. 1. This showed that the sample powder, although unexceptional to the naked eye, revealed its unconventional origin under magnification. Plate like particles were observed with two flat opposing edges, and roughened sides, apparently sections of the original film that had been broken up. The edges of these plates seemed to be consistently about 10 μm apart, and this must correspond to the thickness of the original film. This would give a growth rate of 670 nm min^{-1}, a value consistent with atmospheric pressure chemical vapour deposition [33].

3.2. Diffraction data

Neutron diffraction data were collected by six banks of detectors producing six histograms with an overall d-spacing range of 0.33 Å to 20 Å. The detection of a small amount of iron in the sample by EDX, combined with the previous indication of partially occupied metal sites meant that the structure could not be fully determined by neutron diffraction alone. Iron has a positive neutron scattering length of 9.45 fm, while that of titanium is negative (-2.85 fm). As such in a refinement where both total metal content and the ratio of iron to titanium are being refined, no definite composition for a metal site can be determined. To alleviate this problem, X-ray diffraction data were also recorded in the range of $5° < 2\theta < 100°$ and a combined X-ray-neutron refinement conducted.

An initial structural model was set up to be refined against this data, using the Cmcm space group with lattice parameters $a = 3.804$ Å, $b = 9.648$ Å, and $c = 9.868$ Å, based upon the pseudo-brookite structure already determined from X-ray diffraction data [18]. Additional low intensity Bragg peaks were observed which could be indexed to the anatase polymorph of TiO_2. This was included in the model as a second phase. The lattice parameters and background profile functions of this model were then refined using a Le Bail fitting routine, to determine optimum values for these, independent of a structural model, for all histograms. Using these peak profile and lattice parameters a number of structural models were then set up, based again upon the previously published crystallographic sites and positions – two titanium sites (4c, 8f) and three anion sites (4c, 8f, 8f). In one model all the anion sites were occupied by oxygen, in a second exclusively by nitrogen. These were used as control experiments. In the third

model a nitrogen and an oxygen atom were placed on each of the three anion crystallographic sites, initially each with an occupancy of 50% oxygen and 50% nitrogen, with the isotropic displacement parameter U_{iso} constrained to be the same for the oxygen atom and nitrogen atom sharing each site, although the value was unconstrained between the three anion crystallographic sites. This ratio of oxygen to nitrogen was allowed to refine independently for each site, although the model was constrained such that each anion site remained fully occupied – previous X-ray diffraction work showed no sign of anion site vacancy. In all three models all atom position and isotropic displacement parameters were refined. Additionally the titanium ion site occupancies were refined although the U_{iso} for both ions were constrained to be equal.

Of the three configurations the mixed oxygen–nitrogen model produced the best fit to the data with a χ^2 of 6.0, compared to significantly larger values of 8.4 and 15.7 for the oxygen only and nitrogen only models. The mixed model had values of U_{iso} that were reasonable. The oxygen and nitrogen only models had some anionic U_{iso} values that refined to be unphysically negative in some cases, and in excess of 0.01 Å^2 in others – further reasons to reject them. As such the mixed anion model gave the best and most reliable fit to the data. This mixed anion model was then modified to include 1.6% iron on the metal ion sites to take account of the iron determined to be present using the EDX measurements. The fraction of iron and titanium on each site was then allowed to refine independently. This final model had a marginally better fit with χ^2 of 5.8 compared to the titanium only mixed anion site model of 6.0. Fig. 2 shows a plot of the refined model pattern and collected diffraction data from the 5th neutron diffraction data bank positioned at 91.3° covering a d-spacing range of 0.36–2.7 Å.

The goodness of fit parameters for the final structural model were $\chi^2 = 5.8$ for all databanks and average wRp of 3.9% for the 6 neutron databanks and 2.0% for X-ray databank. In this model based upon the pseudobrookite structure, the occupation of the sites gave a composition of $Ti_{2.92}Fe_{0.01}O_{4.02}N_{0.98}$, with a 2.8% by mass anatase TiO_2 impurity. The quantity of iron found within the structure was 0.4% by metal basis, somewhat lower than that found by EDX analysis of 1.6–1.8%. This discrepancy can be explained by the diffraction analysis determining the iron found throughout the structure, whereas the EDX analysis will be dominated by the surface – a greater concentration of iron would
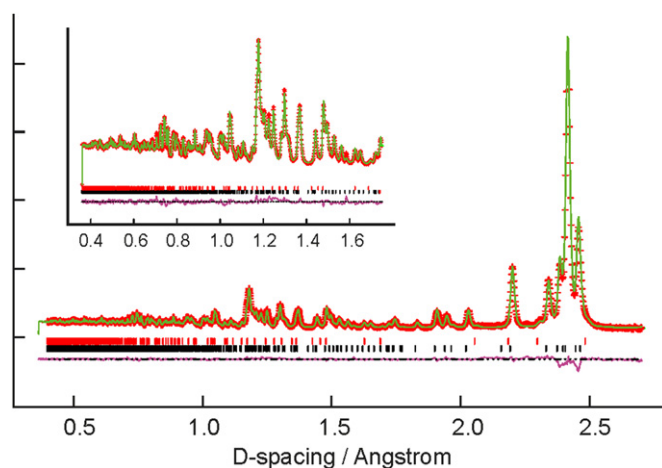

Fig. 2. Neutron diffraction data from the 91.3° detector (bank 5) and refined model pattern. Data is shown in red, refined model in green in difference plot in purple. Black tick marks indicate the indexed peak positions for the unit cell of $Ti_{2.92}Fe_{0.01}O_{4.02}N_{0.98}$, red tick marks indicate anatase polymorph of TiO_2. The inset shows an enlargement of the low d-spacing region of the diffraction pattern.

be expected where the film was grown in contact with the steel surface. The lattice parameters for the principal phase were found to be $a=3.81080(6)$ Å, $b=9.6253(2)$ Å, and $c=9.8859(2)$ Å. Significantly the neutron model gave an oxygen to nitrogen ratio of $\approx 4:1$, this matches that determined previously using XPS [18], and this ratio was allowed to refine completely independently, thus the match is significant. However the oxygen and nitrogen ions are not distributed randomly across the three crystallographic sites. One site is occupied exclusively by oxygen (8f), another is 78% oxygen, 22% nitrogen (also an 8f) while the final site (4c) is 55% nitrogen and 45% oxygen. Table 1 gives the full structural details of the model, and Fig. 3 shows a projection of

Table 1
Structural parameters of the model of $Ti_{2.92}Fe_{0.01}O_{4.02}N_{0.98}$ found in the $Cmcm$ space group with lattice parameters, $a=3.81080(6)$ Å, $b=9.6253(2)$ Å, $c=9.8859(2)$ Å.

Atom site	Wyckoff position	x	y	z	U_{iso} (Å²)	Site occupancy
Ti1	4c	0	0.6975(2)	0.25	0.0019(2)	0.918(4)
Ti2	8f	0	0.6401(1)	0.5656(1)	0.0019(2)	0.998(4)
O1	8f	0	0.18798(6)	0.56711(6)	0.0057(2)	0.780(5)
N1	8f	0	0.18798(6)	0.56711(6)	0.0057(2)	0.220(5)
O2	8f	0	0.54749(8)	0.38290(7)	0.0065(2)	1.0
O3	4c	0	0.73230(6)	0.75	0.0041(2)	0.453(8)
N3	4c	0	0.73230(6)	0.75	0.0041(2)	0.547(8)
Fe1	4c	0	0.6975(2)	0.25	0.0019(2)	0.008(2)
Fe2	8f	0	0.6401(1)	0.5656(1)	0.0019(2)	0.002(2)

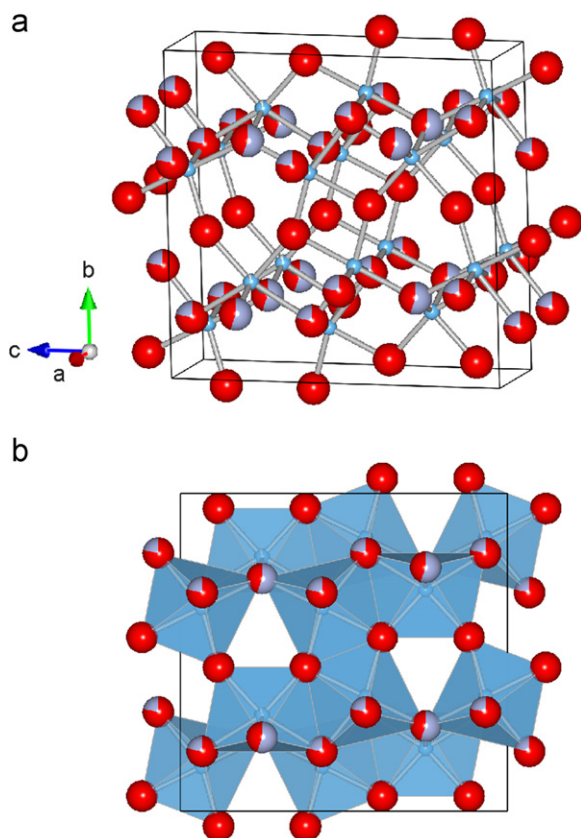**Fig. 3.** (a) Projection tilted from the 100 face showing the unit cell of the $Ti_{2.92}Fe_{0.01}O_{4.02}N_{0.98}$ structural model. The anion sites are represented by the larger spheres and segmented to show the fraction of occupancy by nitrogen (blue–grey) or oxygen (red). The two mixed oxygen–nitrogen sites are in the dense titanium containing layers, while the 3 coordinate linking anion sites are occupied exclusively by oxygen. (b) Projection from the 100 face, with MX_6 polyhedra shown.

the unit cell. The structure contains two cation sites. The 8f metal site is fully occupied, principally by titanium, with 0.2% of iron. All of the cation vacancy is accommodated on the other cation position, the 4c site, which is 92% occupied by titanium and 0.8% occupied by iron, with a 7.4% vacancy.

The structure of $Ti_{2.92}Fe_{0.01}O_{4.02}N_{0.98}$ can be considered as dense sheets of edge sharing MX_6 octahedra, running parallel to the 010 plane which contain the mixed anion O/N1 and O/N3 sites in which the anion is four-coordinate to titanium. These dense sheets are linked by the third anion site, O2, with the MX_6 octahedra sharing a mixture of edges and vertices. The linking O2 anion site is exclusively occupied by oxygen, and is only three-coordinate to titanium. This is consistent with Paulings 2nd rule, where the higher charge N^{3-} ions will by preference occupy sites with higher coordination [34]. This is also the same pattern that is observed in β-TaON, adopting the baddeleyite structure and γ–TaON with the VO_2(B)-type structure, where the nitrogen preferentially occupies the 4 coordinate site over the 3 or 2 coordinate anion sites also available in these structures [14,15]. The bond lengths for each of the cation and anion environments is shown in table 2, and from this can be seen a large variation in Ti–O/N bond lengths, with a difference of 12% between the longest and shortest Ti–O/N distances. However, this variation is typical for the pseudobrookite structure, with the equivalent difference in length being 17% in the analogous $V_3O_{4.61}N_{0.27}$ vanadium oxynitride [19]. This variation can be accounted for by the differences in each of the coordination environments. The shortest distances are to the 3 coordinate O2 site, connecting polyhedra which are corner sharing only. The longest distances are from the metal sites to the O/N1 site, which has the most edge sharing polyhedra – as such the variation can be accounted for by the repulsion between the titanium ions [35].

3.3. Thermodynamic stability

The tests of the stability of $Ti_{2.92}Fe_{0.01}O_{4.02}N_{0.98}$ at elevated temperatures in air found that the material was stable at 300 °C, but at 400 °C and above the sample oxidised to the rutile polymorph of TiO_2. Similar experiments conducted under vacuum found that the region of stability was extended to 600 °C, but at 700 °C and above the material decomposed to TiN and TiO_2. These results provide a limit on the parameters for the synthesis of this metastable oxynitride by more conventional solid state synthetic

Table 2
Bond lengths for the metal-anion bonds in the structure of $Ti_{2.92}Fe_{0.01}O_{4.02}N_{0.98}$.

Ti1 Environment	Bond length (Å)
Ti1–O/N1 (×2)	2.118(1)
Ti1–O2 (×2)	1.951(2)
Ti1–O/N3 (×2)	2.022(1)
Ti2 Environment	**Bond length (Å)**
Ti2–O/N1 (×2)	1.9604(3)
Ti2–O/N1	2.112(1)
Ti2–O2	2.014(2)
Ti2–O2	1.876(1)
Ti2–O/N3	2.028(1)
O/N1 Environment	**Bond length (Å)**
O/N1–Ti1	2.118(1)
O/N1–Ti2	2.112(1)
O/N1–Ti2 (×2)	1.9604(3)
O2 Environment	**Bond length (Å)**
O2–Ti1	1.951(2)
O2–Ti2	2.014(2)
O2–Ti2	1.876(1)
O/N3 Environment	**Bond length (Å)**
O/N3–Ti2 (×2)	2.028(1)
O/N3–Ti1 (×2)	2.022(1)

methods, which typically use temperatures of 900–1200 °C. A similar result has been found by Nakhal et al. working on a vanadium oxynitride, $V_3O_{4.61}N_{0.27}$, also synthesised at low temperature and also isostructural to pseudobrookite. They found that the oxynitride decomposed to oxides under inert gas at 630 °C and to V_2O_5 in air at 350 °C [19]. These combined results indicate that the use of lower temperatures and non-oxide precursors can allow access to previously unknown, kinetically stable phases, and is perhaps a fruitful route for further investigations.

4. Conclusion

It has been possible to synthesise a 0.7 g powder sample of $Ti_{2.92}Fe_{0.01}O_{4.02}N_{0.98}$ by delamination of a thin film from a steel substrate grown by atmospheric pressure chemical vapour deposition. Although this led to a small contamination of the material with iron, the large sample size allowed a neutron diffraction experiment to be carried out. This revealed partial oxygen nitrogen ordering, with an uneven distribution of nitrogen across the anion sites. In particular the preference of nitrogen for higher coordination sites was noted, with the only 3 coordinate anion site being exclusively occupied by oxygen. It was also identified that the oxynitride was not stable above 700 °C, but instead is a kinetic product requiring low temperature synthesis, in this case through reaction of $TiCl_4$ with sources of oxygen and nitrogen.

References

[1] G. Hyett, N. Barrier, S.J. Clarke, J. Hadermann, J. Am. Chem. Soc. 129 (2007) 11192–11201.
[2] S.J. Clarke, P. Adamson, S.J.C. Herkelrath, O.J. Rutt, D.R. Parker, M.J. Pitcher, C.F. Smura, Inorg. Chem. 47 (2008) 8473–8486.
[3] S.H. Elder, F.J. DiSalvo, L. Topor, A. Navrotsky, Chem. Mater. 5 (2002) 1545–1553.
[4] A. Fuertes, Dalton Trans. 39 5942–5948.
[5] Y. Kamihara, T. Watanabe, M. Hirano, H. Hosono, J. Am. Chem. Soc. 130 (2008) 3296–3297.
[6] D. Logvinovich, Stefan G. Ebbinghaus, A. Reller, I. Marozau, D. Ferri, A. Weidenkaff, Z. Anorg. Allg. Chem. 636 (2010) 905–912.
[7] S.G. Ebbinghaus, H.-P. Abicht, R. Dronskowski, T. Mueller, A. Reller, A. Weidenkaff, Prog. Solid State Chem. 37 (2009) 173–205.
[8] S.J. Clarke, K.A. Hardstone, C.W. Michie, M.J. Rosseinsky, Chem. Mater. 14 (2002) 2664–2669.
[9] R. Marchand, Y. Laurent, J. Guyader, P. L'Haridon, P. Verdier, J. Eur. Ceram. Soc. 8 (1991) 197–213.
[10] B. Wang, B.C. Chakoumakos, B.C. Sales, J.B. Bates, J. Solid State Chem. 122 (1996) 376–383.
[11] R. Kiessling, L. Peterson, Acta Metall. 2 (1954) 675–679.
[12] N. Schonberg, Acta Chem. Scand. 8 (1954) 208–212.
[13] S.J. Clarke, C.W. Michie, M.J. Rosseinsky, J. Solid State Chem. 146 (1999) 399–405.
[14] D. Armytage, B.E.F. Fender, Acta Crystallogr., Sect. B: Struct. Sci 30 (1974) 809–812.
[15] H. Schilling, A. Stork, E. Irran, H. Wolff, T. Bredow, R. Dronskowski, M. Lerch, Angew. Chem. Int. Ed. 46 (2007) 2931–2934.
[16] N. Suliman, L. Marck-Willem, B. Thomas, D. Richard, L. Martin, Z. Anorg. Allg. Chem. 636 1006–1012.
[17] T. Bredow, M. Lerch, Z. Anorg. Allg. Chem. 633 (2007) 2598–2602.
[18] G. Hyett, M.A. Green, I.P. Parkin, J. Am. Chem. Soc. 129 (2007) 15541–15548.
[19] S. Nakhal, W. Hermes, T. Ressler, R. Pöttgen, M. Lerch, Z. Anorg. Allg. Chem. 635 (2009) 2016–2020.
[20] G. Hyett, M.A. Green, I.P. Parkin, J. Photochem. Photobiol., A 203 (2009) 199–203.
[21] A. Salamat, G. Hyett, R.Q. Cabrera, P.F. McMillan, I.P. Parkin, J. Phys. Chem. C 114 (2010) 8546–8551.
[22] M. Onoda, J. Solid State Chem. 136 (1998) 67–73.
[23] M. Onoda, Y. Ogawa, K. Taki, J. Phys. Condens. Matter 10 (1998) 7003–7013.
[24] I.E. Grey, J. Ward, J. Solid State Chem. 7 (1973) 300–307.
[25] I.E. Grey, C. Li, I.C. Madsen, J. Solid State Chem. 113 (1994) 62–73.
[26] H.J. Steiner, X. Turrillas, B.C.H. Steele, J. Mater. Chem. 2 (1992) 1249–1256.
[27] S.J. Clarke, B.P. Guinot, C.W. Michie, M.J.C. Calmont, M.J. Rosseinsky, Chem. Mater. 14 (2001) 288–294.
[28] F. Pors, R. Marchand, Y. Laurent, P. Bacher, G. Roult, Mater. Res. Bull. 23 (1988) 1447–1450.
[29] E. Gunther, R. Hagenmayer, M. Jansen, Z. Anorg. Allg. Chem. 626 (2000) 1519–1525.
[30] A.C. Hannon, Nucl. Instrum. Methods Phys. Res., Sect. A 551 (2005) 88–107.
[31] B.H. Toby, J. Appl. Crystallogr. 34 (2001) 210–213.
[32] A.C. Larson, R.B. Von Dreele, Los Alamos Nat. Lab. Rep. LAUR (2000) 86–748.
[33] G. Hyett, R. Binions, I.P. Parkin, Chem. Vap. Deposition 13 (2007) 675–679.
[34] L. Pauling, J. Am. Chem. Soc. 51 (1929) 1010–1026.
[35] S. Asbrink, Acta Crystallogr., Sect. B: Struct. Sci 36 (1980) 1332–1339.